PHYSICAL REVIEW B **88**, 060408(R) (2013)

Probing magnetic order in $CuFeO_2$ through nuclear forward scattering in high magnetic fields

C. Strohm,[1,*] T. T. A. Lummen,[2] I. P. Handayani,[2] T. Roth,[1] C. Detlefs,[1] P. J. E. M. van der Linden,[1] and P. H. M. van Loosdrecht[2,†]

[1]*European Synchrotron Radiation Facility, BP 220, 38043 Grenoble, France*

[2]*Zernike Institute for Advanced Materials, University of Groningen, Nijenborgh 4, 4974 AG Groningen, The Netherlands*

(Received 17 August 2012; revised manuscript received 14 June 2013; published 26 August 2013)

Determining the magnetic order of solids in high magnetic fields is technologically challenging. Here we probe the cascade of magnetic phase transitions in frustrated multiferroic $CuFeO_2$ using nuclear forward scattering (NFS) in pulsed magnetic fields up to 30 T. Our results are in excellent agreement with detailed neutron diffraction experiments, currently limited to 15 T, while providing experimental confirmation of the proposed higher field phases for both $H \parallel c$ and $H \perp c$. We thus establish NFS as a valuable tool for spin structure studies in very high fields, both complementing and expanding on the applicability of existing techniques.

DOI: 10.1103/PhysRevB.88.060408 PACS number(s): 75.25.−j, 75.10.Jm, 75.50.Bb, 76.80.+y

Geometric frustration and anisotropy lead to distinct types of magnetic order when the magnetic exchange interaction becomes comparable to other energy scales at sufficiently low temperatures. In $CuFeO_2$ (CFO), manifestations of both are observed and intricately related. The application of a magnetic field tunes the balance between the interactions and successively selects metamagnetic phases where various spin structures (SSs) minimize the total energy of the system.

In CFO (space group $R\bar{3}m$, $a,b = 3.03$ Å, $c = 17.17$ Å), Fe^{3+} ions are antiferromagnetically coupled on triangular lattice planes, separated by layers of O^{2-} and Cu^{1+} ions.[1] From the lattice geometry one would expect geometric frustration and from the Heisenberg nature of the Fe spins ($3d^5$, $S = 5/2$, $L = 0$) a noncollinear 120° spin configuration. However, when CFO is cooled it undergoes two successive phase transitions at $T_{N1} = 14$ K and $T_{N2} = 11$ K from the high-temperature paramagnetic phase into a collinear antiferromagnetic phase,[2] reminiscent of systems with an Ising-type anisotropy. At the same time, the lattice symmetry is lowered from hexagonal to monoclinic through a scalene distortion.[3] Upon application of a magnetic field in the ordered phase, CFO exhibits a cascade of magnetic phase transitions before reaching saturation at about 80 T.[4] For $H \parallel c$, CFO undergoes three first order transitions, leading to a plateau at 1/3 of the saturation magnetization (Fig. 1). The first field-induced phase shows electric polarization[5] and a linear increase in the magnetization, whereas the second field-induced phase is a plateau at 1/5 of the saturation magnetization. For $H \perp c$ the magnetization grows linearly before similarly halting at a 1/3 plateau following a first order transition. For both orientations, this plateau is delimited to higher fields by a second order transition, after which the magnetization first rises with different slopes before the curves eventually become indistinguishable after one last common first order transition at 53 T.[6]

The association of the scalene lattice distortion observed in the low-temperature, low-field phase with a spin-driven analog of the Jahn-Teller effect gives a first hint on the true origin of the observed highly anisotropic behavior.[3] A further clue comes from the release of these distortions with increasing magnetization of the sample.[7–9] The inclusion of a biquadratic term to describe the spin-lattice coupling finally allowed to understand the observed field dependent easy axis anisotropy and the last metamagnetic transition at 53 T, where the undistorted lattice and isotropic behavior are recovered.[6,10,11] Probing the SSs is of particular importance to test any theory describing the magnetization process in CFO. After Mössbauer experiments[2] had identified collinear antiferromagnetic order below T_{N2}, a series of neutron scattering experiments to determine the spin structures was performed. The present picture is that, for $T_{N2} < T < T_{N1}$, CFO is in a partially disordered incommensurate state with a sinusoidally amplitude modulated, temperature dependent propagation vector $(q,q,0)$, $0.19 \leqslant q \leqslant 0.22$,[12,13] before ordering in the collinear four-sublattice (4sl) $(\frac{1}{4},\frac{1}{4},\frac{3}{2})$ state below T_{N2}. Much effort went into the study of the phase $H_{c1}^{\parallel} \leqslant H \leqslant H_{c2}^{\parallel}$ for which a proper helical SS with an incommensurate wave vector was proposed,[14] in order to account for the multiferroic behavior. This model was corroborated through studies of CFO samples with partial substitution of Fe through Al or Ga for which the ferroelectric state could be stabilized at zero field.[15–18] The plateau for $H_{c2}^{\parallel} \leqslant H \leqslant H_{c3}^{\parallel}$ at 1/5th of the saturation magnetization was determined to be a 5sl SS with $\left(\frac{1}{5},\frac{1}{5},0\right)$.[14] For the application of $H \perp c$ it was found that the 4sl state remains stable up to 14.5 T while the moments cant slightly towards the applied field.

The direct observation of the SS in the high-field phases through neutron diffraction or x-ray magnetic scattering experiments remains extremely difficult. Both methods require long integration times and large solid angles which are difficult to obtain in combination with the high magnetic fields needed to reach these phases. While exploratory neutron diffraction experiments could observe a three-sublattice reflection at the 1/3 plateau,[19,20] x-ray magnetic scattering in high fields has only recently been demonstrated for the first time.[21]

In this Rapid Communication we report on the use of nuclear forward scattering (NFS) of synchrotron radiation from the Mössbauer isotope ^{57}Fe ($E_0 = 14.413$ keV, $\tau_0 = 141$ ns, $1/2 \rightarrow 3/2$ $M1 + E2$) in pulsed magnetic fields (PMFs) to probe the SS of the metamagnetic phases of CFO in fields up to 25 T for $H \parallel c$ and 30 T for $H \perp c$. Our model-based analysis is in excellent agreement with the well-known low-field spin structures and provides experimental verification of proposed

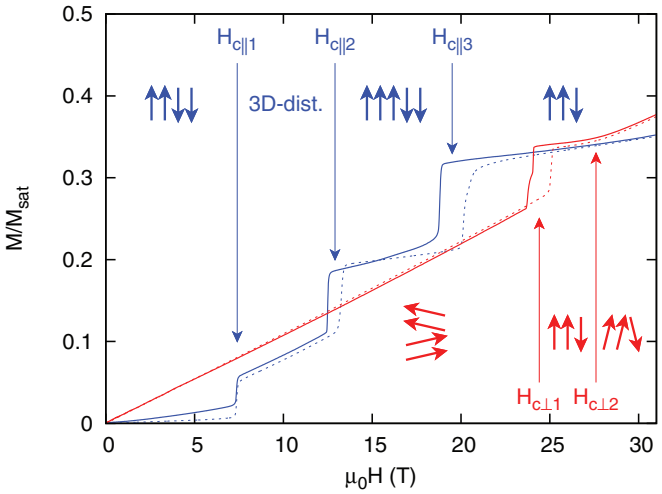

FIG. 1. (Color online) Bulk magnetization measurements of $CuFeO_2$ at 4.2 K (for data and details, see Ref. 11). Blue line: $H \parallel c$; red line: $H \perp c$. Dashed lines: Rising field; solid lines: falling field. Transition fields and the corresponding model spin structures are indicated by arrows.

higher-field structures, thus demonstrating the feasibility of the technique for the study of spin structures in very high fields.

In NFS, nuclear levels split by hyperfine interactions are excited simultaneously by a pulsed synchrotron source, tuned close to the resonance energy. The time dependence of the subsequent decay exhibits a characteristic beat pattern resulting from the interference between different transitions. Even though NFS cannot directly resolve spin structures, relevant information for the comparison of model-based calculations of the time spectra is obtained.[22] NFS probes the spin structure in several ways: (i) Through the selection rules, the transition probability is determined by the relative orientation of the quantizing field and the polarization of the incident beam. (ii) The total internal magnetic field H_{int} probed by NFS is the vector sum of the applied field, the field generated by the atomic moment, and the transferred hyperfine and demagnetizing fields. The internal field at a given site thus contains information about its orientation with respect to the applied field. (iii) In the presence of different sites, additional frequencies arise in the decay from intersite interference depending on the geometry. Further beats arise from the interaction of the nuclear quadrupole moment with the electric field gradient and from the optical thickness of the sample, leading to complex hybrid beat patterns.

A single crystal of CFO was grown by the floating zone method following Ref. 1. Part of the sample was enriched in ^{57}Fe through insertion of a small ^{57}Fe-enriched section into the large polycrystalline template before growing the crystal in a mirror image furnace. The crystal was characterized through Mössbauer spectroscopy and magnetization measurements.[6,11] The former did not show traces of magnetic impurities and the phase diagrams obtained through the latter agree well with previous work.

The enriched crystal section was located by nuclear fluorescence and the enrichment was found to be $\geqslant$90% in the NFS measurements. The samples were oriented to within $\pm 2^\circ$, polished to a thickness of 48 ± 2 μm for $k \parallel c$ and to 36 ± 6 μm for $k \perp c$, glued onto 155 μm diamond substrates, and mounted directly in the He flow of the sample cryostat of the PMF setup used in the experiment. The magnetic field was always applied along the beam. In order to attain the 1/3 plateau for $H \parallel c$ and $H \perp c$ we use a miniature pulsed field coil providing fields up to 30 T at repetition rates of 6 min^{-1}.[23] The system features an independent sample cryostat and the sample temperature was kept at 5 ± 0.5 K. The NFS experiments were carried out at the beamline ID18 in 16-bunch timing-mode operation of the ESRF. A detailed description of the experimental setup and detection scheme for NFS in PMF is given in Ref. 24. The count rates were typically 25 kHz for $H \parallel c$ and 35 kHz for $H \perp c$ in the time window from 12 to 176 ns at an average storage ring current of 70 mA.

Figure 2 (top) shows the experimental raw data for two different orientations of the crystallographic c axis with respect to the applied field. For $H \perp c$ two geometries were measured to better constrain the spin orientations: c parallel and perpendicular to the magnetic polarization vector $\mathbf{e}_m$ of the incident beam, respectively. Each data point represents a photon count. The simultaneous acquisition and continuity of the data in the applied field allows the direct visual observation of the different phases. For $H \parallel c$ we observe three first order metamagnetic transitions accompanied by large hysteresis at $H_{c1}^{\parallel} = 7.3$ T ($H_{c1}^{\parallel} = 7.1$ T), $H_{c2}^{\parallel} = 13.4$ T ($H_{c2}^{\parallel} = 12.5$ T), and $H_{c3}^{\parallel} = 20.3$ T ($H_{c3}^{\parallel} = 19.1$ T) in increasing (decreasing) field. For $H \perp c$ there is one first order transition at $H_{c1}^{\perp} = 25.4$ T ($H_{c1}^{\perp} = 24.3$ T) in increasing (decreasing) field. All transition fields agree with previous work. For a quantitative evaluation, the data was binned into appropriate field regions within each phase, in order to obtain the NFS time spectra shown in Fig. 3. The spectra were fitted using the MOTIF package,[25] using a model-based approach, making assumptions on the spin structure while fitting selected parameters for each site in order to adjust the calculated spectrum to the experiment.

Figure 3 (top) a shows selected time spectra along with the fits to the data. The zero-field spectra for $H \perp c$ for two orientations of the crystallographic c axis with respect to $\mathbf{e}_m$ allow to constrain the sublattice magnetizations and the principal axis of the electric field gradient ($\mathbf{v}_{zz}$) along c, whereas the presence and amplitude of intersite interferences for $H \parallel c$ confirms the antiferromagnetic alignment of the sublattices. The values of 51.5 T for the magnetic hyperfine field and $6.5\Gamma_0$ for the quadrupole splitting agree with previous work.[2] Figure 3(a) (top) shows the spectra for $H \parallel c$. In order to fit the collinear phases for $H < H_{c1}^{\parallel}$ (4sl: $\uparrow\uparrow\downarrow\downarrow$), $H_{c2}^{\parallel} < H < H_{c3}^{\parallel}$ (5sl: $\uparrow\uparrow\uparrow\downarrow\downarrow$) and $H_{c3}^{\parallel} < H < H_{\text{max}}$ (3sl: $\uparrow\uparrow\downarrow$), we assume two sites, one parallel to and one opposite to the applied field, and fit the respective internal fields and relative weight, whereas the quadrupole splitting (QS) was variable but constrained to be equal for both sites. The internal fields reported at the bottom of Fig. 3(a) evolve strictly linear with H, as expected for a parallel and antiparallel alignment of the sites with the applied field, whereas the relative weight of the sites reflects the 4sl, 5sl, and 3sl structures. The QS (not shown) does not vary significantly throughout the different

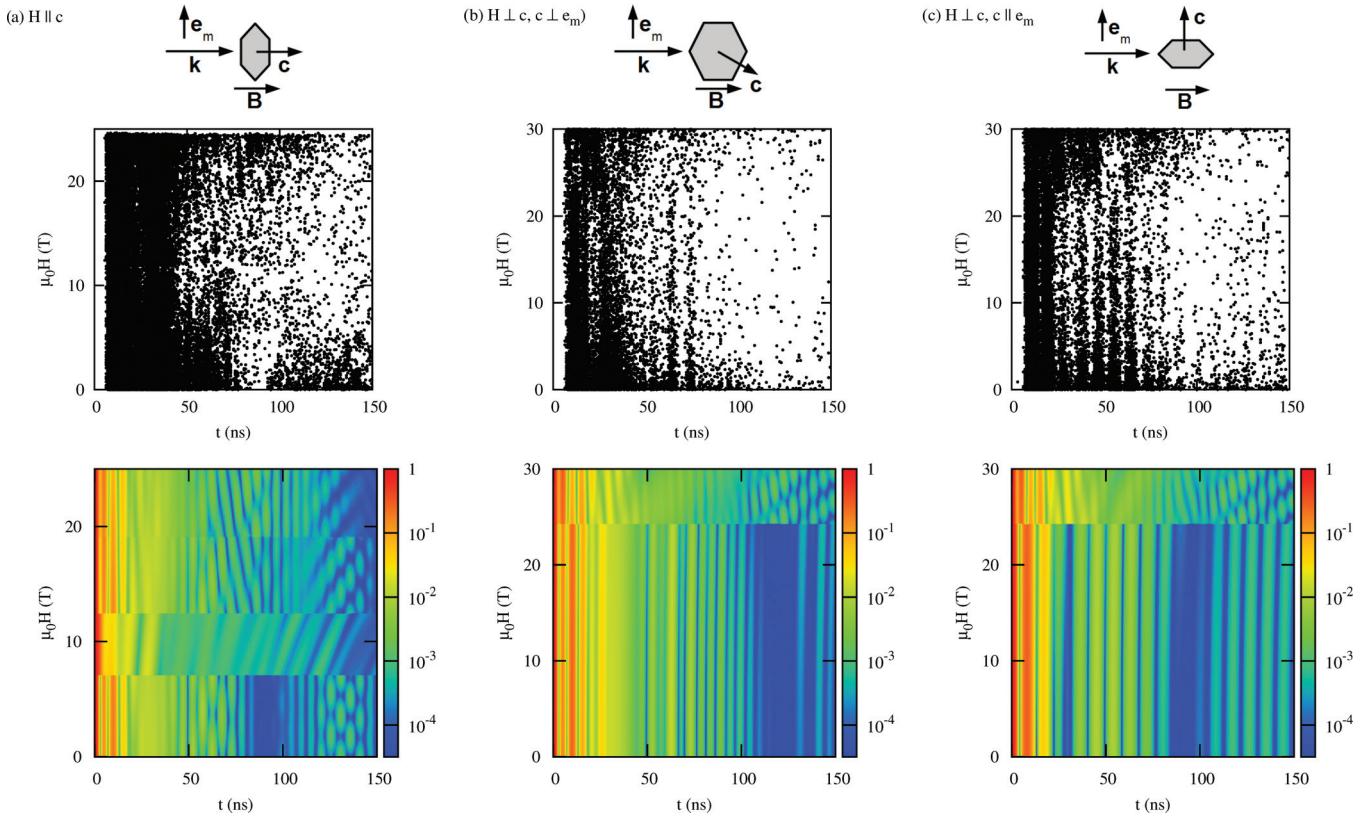

FIG. 2. (Color online) NFS intensity, as a function of field and delay. Top: Experimentally observed events for different sample orientations. (a) $H \parallel c$, (b) $H \perp c$ and $c \perp e_m$, and (c) $H \perp c$ and $c \parallel e_m$. Bottom: Simulation of the NFS intensity using simple model structures (see the text and Fig. 1).

phases. The sublattices within the 5sl and 3sl structures are in principle required to be of different symmetry, but the present data do not warrant fitting their QS independently. For $H_{c1}^{\parallel} < H < H_{c2}^{\parallel}$ we have tried to fit two spin structures compatible with the observation of ferroelectricity in this phase. A cycloid structure, where the spins are slightly canted away from the *a*-*b* plane, and a transverse proper helix structure. While the cycloid structure does not allow to fit the data with acceptable values for the canting angle and internal fields as the only fitting parameters, we could reproduce prominent features of the data with a three-dimensional (3D) distribution approximating equally distributed domains of propagation vectors.

For $H \perp c$ we have measured two orientations of the c axis with respect to $\mathbf{e}_m$. Due to the selection rules only the $\Delta m \pm 1$ transitions are excited for $\mathbf{m} \perp \mathbf{e}_m$ whereas only the $\Delta m = 0$ transitions are probed for $\mathbf{m} \parallel \mathbf{e}_m$. The different quantum beat periods visible in Figs. 3(b) and 3(c) thus directly evidence the orientation of the sublattice magnetizations parallel to c and prove the stability of the canted phase up to $H_{c1}^{\perp}$. As a function of field the canting of the spins at the origin of the linear increase of the bulk magnetization amounts to 11.5° (with respect to the c axis) at 20 T and leads only to a small variation of the value (and angle) of the resulting internal field. Above $H_{c1}^{\perp}$, the spectra change abruptly and are best fitted with two sites aligned parallel and antiparallel to the applied field and a relative weight of 2:1, which corresponds to a collinear three-sublattice structure. Assuming a fraction of spins that remains pinned along c, and is decreasing with field, improved the fit for $\mathbf{c} \parallel \mathbf{e}_m$. The differences in the spectra for the 1/3 plateau between Figs. 3(a) and 3(b) result mainly from the different sample thickness, whereas the different orientation of $\mathbf{v}_{zz}$ with respect to $\mathbf{e}_m$ is at the origin of the differences between Figs. 3(b) and 3(c). The values of the internal fields H_{int} and their angles with respect to the c axis used to fit the spectra for $H \perp c$ are reported in the lower panels of Figs. 3(b) and 3(c). The bottom panels in Fig. 2 show a calculation of the NFS intensity using the relevant model parameters of the fits described above. The calculation and the experimental point density are related through the acquisition time per field interval.

In conclusion, this experiment represents an application of NFS in high magnetic fields up to 30 T for the study of spin structures, where other more direct methods such as neutron diffraction and x-ray magnetic scattering face severe challenges due to their requirement of large solid angles. The low-field data and all transition fields are in good agreement with previous work. For $H \leqslant H_{c1}^{\parallel}$ and $H_{c2}^{\parallel} \leqslant H \leqslant H_{c3}^{\parallel}$ we confirm the collinear spin structures parallel to the crystallographic c axis. The data for the ferroelectric phase for $H_{c1}^{\parallel} \leqslant H \leqslant H_{c2}^{\parallel}$ does not support the cycloid structure, while a 3D distribution approximating a multidomain transverse proper helix structure gives qualitative agreement. For the plateau at 1/3 of the saturation magnetization we find that a collinear spin arrangement corresponding to the expected

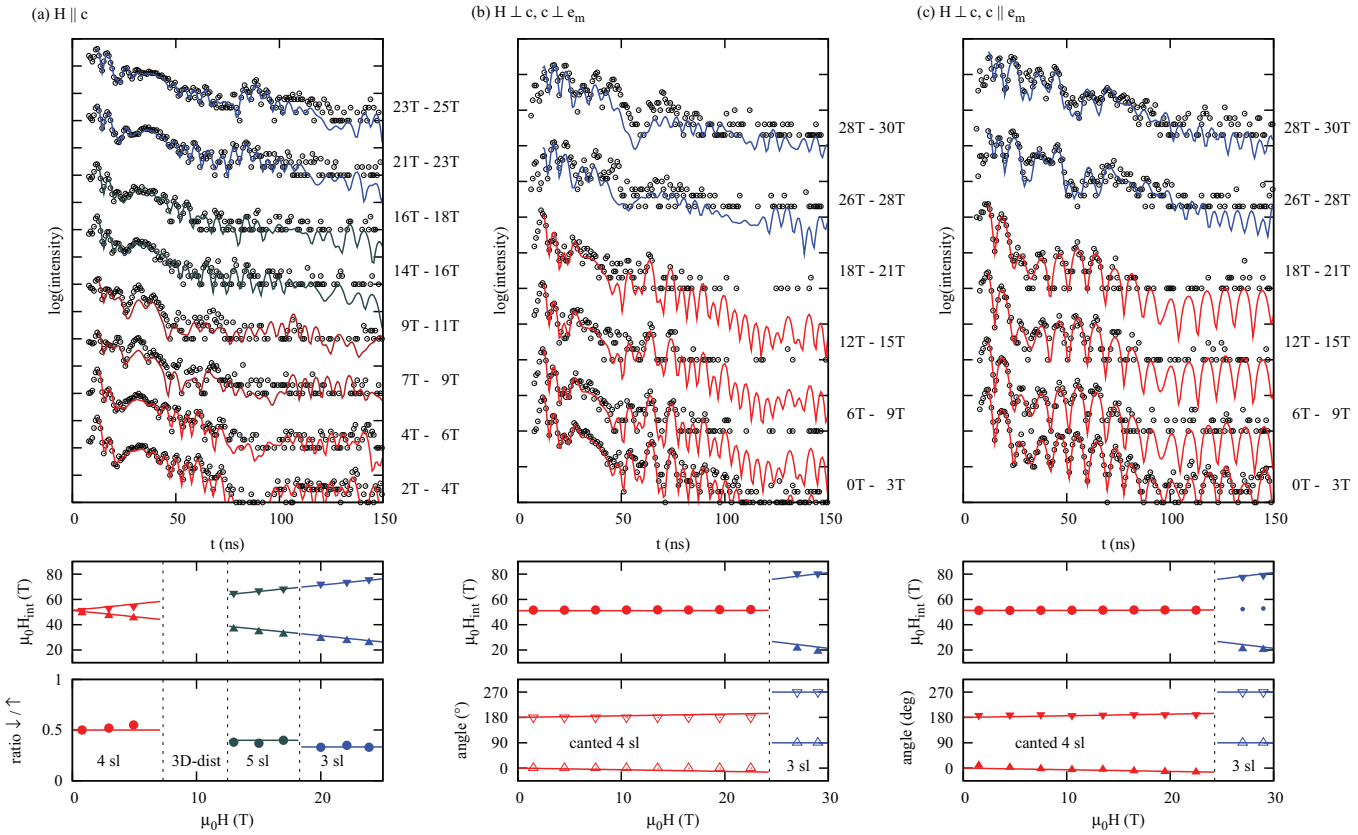

FIG. 3. (Color online) NFS time spectra, fits, and model parameters for different sample orientations. (a) $H \parallel c$, (b) $H \perp c$ and $c \perp e_m$, and (c) $c \parallel e_m$. Top: NFS intensity as a function delay. The spectra were extracted from Fig. 2 through binning in time (0.8 ns) and field. Line: Fit to the data. Bottom: Points are model parameters. Solid symbols: Values obtained from the fits of the time spectra; open symbols: fixed parameters; lines: parameters used in the simulations in the lower panels of Fig. 2.

three-sublattice structure best represents the data above $H_{c3}^{\parallel}$. For $H \perp c$ we directly evidence the stability of the canted four-sublattice phase in the plane defined by H and c up to $H_{c1}^{\perp}$. In the 1/3 plateau, a collinear three-sublattice configuration provides the best fit, if a fraction of spins pinned along the c axis is allowed for. At the moment the development of a pulsed field coil with perpendicular access is underway. In combination with full polarization control using diamond phase plates, this would greatly simplify the interpretation of the spectra resulting from complex spin structures in the future and facilitate ruling out ambiguities.

The authors gratefully acknowledge A. Nugroho for assistance with the sample growth, F. E. Wagner for characterizing the samples through Mössbauer spectroscopy, and A. I. Chumakov for help at the beamline.

*cornelius.strohm@esrf.fr
†p.h.m.van.loosdrecht@rug.nl

[1]T. R. Zhao, M. Hasegawa, and H. Takei, J. Cryst. Growth **166**, 408 (1996).
[2]A. H. Muir and H. Wiedersich, J. Phys. Chem. Solids **28**, 65 (1967).
[3]N. Terada, S. Mitsuda, H. Ohsumi, and K. Tajima, J. Phys. Soc. Jpn. **75**, 023602 (2006).
[4]Y. Ajiro, T. Asano, T. Takagi, M. Mekata, H. A. Katori, and T. Goto, Physica B **201**, 71 (1994).
[5]T. Kimura, J. C. Lashley, and A. P. Ramirez, Phys. Rev. B **73**, 220401 (2006).
[6]T. T. A. Lummen, C. Strohm, H. Rakoto, A. A. Nugroho, and P. H. M. van Loosdrecht, Phys. Rev. B **80**, 012406 (2009).
[7]N. Terada, Y. Tanaka, Y. Tabata, K. Katsumata, A. Kikkawa, and S. Mitsuda, J. Phys. Soc. Jpn. **75**, 113702 (2006).
[8]N. Terada, Y. Narumi, K. Katsumata, T. Yamamoto, U. Staub, K. Kindo, M. Hagiwara, Y. Tanaka, A. Kikkawa, H. Toyokawa, T. Fukui, R. Kanmuri, T. Ishikawa, and H. Kitamura, Phys. Rev. B **74**, 180404(R) (2006).
[9]N. Terada, Y. Narumi, Y. Sawai, K. Katsumata, U. Staub, Y. Tanaka, A. Kikkawa, T. Fukui, K. Kindo, T. Yamamoto, R. Kanmuri, M. Hagiwara, H. Toyokawa, T. Ishikawa, and H. Kitamura, Phys. Rev. B **75**, 224411 (2007).
[10]F. Wang and A. Vishwanath, Phys. Rev. Lett. **100**, 077201 (2008).
[11]T. T. A. Lummen, C. Strohm, H. Rakoto, and P. H. M. van Loosdrecht, Phys. Rev. B **81**, 224420 (2010).

[12]M. Mekata, N. Yaguchi, T. Takagi, T. Sugino, S. Mitsuda, H. Yoshizawa, N. Hosoito, and T. Shinjo, J. Phys. Soc. Jpn. **62**, 4474 (1993).

[13]S. Mitsuda, N. Kasahara, T. Uno, and M. Mase, J. Phys. Soc. Jpn. **67**, 4026 (1998).

[14]S. Mitsuda, M. Mase, K. Prokes, H. Kitazawa, and H. A. Katori, J. Phys. Soc. Jpn. **69**, 3513 (2000).

[15]T. H. Arima, J. Phys. Soc. Jpn. **76**, 073702 (2007).

[16]T. Nakajima, S. Mitsuda, S. Kanetsuki, K. Prokes, A. Podlesnyak, H. Kimura, and Y. Noda, J. Phys. Soc. Jpn. **76**, 043709 (2007).

[17]T. Nakajima, S. Mitsuda, S. Kanetsuki, K. Tanaka, K. Fujii, N. Terada, M. Soda, M. Matsuura, and K. Hirota, Phys. Rev. B **77**, 052401 (2008).

[18]N. Terada, T. Nakajima, S. Mitsuda, H. Kitazawa, K. Kaneko, and N. Metoki, Phys. Rev. B **78**, 014101 (2008).

[19]S. Mitsuda, S. Suzuki, H. Nojiri, M. Motokawa, and M. Arai, KENS Annu. Rep. **10**, 230 (1999/2000).

[20]K. Ohyama, in *SPIN100T* (2007), http://spin100.imr.tohoku.ac.jp/highmagneticfieldspinsciencenewsno6.pdf.

[21]T. Inami, K. Ohwada, Y. H. Matsuda, Z. W. Ouyang, H. Nojiri, T. Matsumura, D. Okuyama, and Y. Murakami, J. Phys. Soc. Jpn. **78**, 033707 (2009).

[22]R. Röhlsberger, H. Thomas, K. Schlage, E. Burkel, O. Leupold, and R. Rüffer, Phys. Rev. Lett. **89**, 237201 (2002).

[23]P. J. E. M. van der Linden, O. Mathon, C. Strohm, and M. Sikora, Rev. Sci. Instrum. **79**, 075104 (2008).

[24]C. Strohm, P. Van der Linden, and R. Ruffer, Phys. Rev. Lett. **104**, 087601 (2010).

[25]Y. V. Shvyd'ko, Hyperfine Interact. **125**, 173 (2000).